International Journal of Refrigeration 168 (2024) 688–695

Contents lists available at ScienceDirect

International Journal of Refrigeration

journal homepage: www.elsevier.com/locate/ijrefrig

Experimental study of the performance of a water-to-water heat pump equipped with a liquid receiver with different charge levels

Etude expérimentale des performances d'une pompe à chaleur équipée d'un réservoir de liquide avec différentes niveaux de charge

Chiara D'Ignazi *, Luca Molinaroli, Carla Bongiorno

Dipartimento di Energia, Politecnico di Milano, Via Lambruschini 4, 20156, Milano, Italy

A R T I C L E I N F O

Keywords:
Charge
Experimental results
Heat pump
Liquid receiver
Refrigerant leakages

Mots clés:
Charge
Fuites de refrigerant
Pompe à chaleur
Récepteur de liquide
Résultats expérimentaux

A B S T R A C T

This paper presents an experimental investigation of the effects of a decreasing refrigerant charge on the performance and operating conditions of an R513A water-to-water heat pump equipped with a large liquid receiver, an electronic expansion valve, and a vapor accumulator at the compressor inlet. The mass of the refrigerant inside the machine is progressively extracted to simulate refrigerant leakages occurring during the normal operation or in case of failures. The results show that the subcooling is the parameter mostly affected by a refrigerant charge variation since it rapidly collapses to 0 K with the charge reduction. Furthermore, it is possible to identify three different zones in which almost all the properties analyzed (COP, heating capacity, operating pressures and expansion valve opening) exhibit peculiar trends with the charge decrease: subcooling sensitivity zone, constant parameters zone, and compressor failure risk zone. The extension of these zones is determined by the size of the liquid receiver which is installed in the system and, for the heat pump under consideration, is between 100% and 95% of the initial charge for the first zone, between 95% and 40% for the second zone, and below 40% for the third zone.

1. Introduction

The Paris Agreement (United Nations Framework Convention on Climate Change, 2015) set off the commitment of the signatory countries, including EU member states, to contain global warming to within 2 K from pre-industrial levels and at least within 1.5 K by mid-century. Air conditioning in residential buildings plays a crucial role in a carbon-neutral transition. According to European estimates, buildings are responsible for 36% of the EU greenhouse gas (GHG) emissions and 40% of energy consumption (European Commission, 2020).

Nowadays, heat pumps represent a potentially effective solution to reduce GHG emissions since it is a technology with low CO_2 emissions for each unit of thermal energy supplied. The considerable diffusion of heat pumps has led to studies aimed at maximizing their performance and minimizing the chance of breakdowns. One of the most common causes of performance degradation is the non-optimal refrigerant charge in the system (Du et al., 2016), which could be due to an improper installation of the machine or refrigerant leakages. Several studies about the refrigerant charge effect on the Coefficient of Performance (COP), the heating capacity and the power absorbed by the compressor of machines without a liquid receiver are documented in the available literature. Houcek and Thedford (1984) were the first to study the effect of overcharging and undercharging on a split air conditioning system equipped with a capillary tube. They showed that a refrigerant overcharge results in a slight increase of the system capacity but causes an increase in electrical demand, while an undercharge condition causes a reduction in the capacity and, consequently, a decrease in performance. Various experimental studies investigated the effect of refrigerant charge with different expansion devices. Grace et al. (2005) showed how a machine equipped with either a thermostatic expansion valve (TEV) or an electronic expansion valve (EXV) can work in a wide range of charge levels, within 75% to 125% of the nominal charge value, with a negligible impact on performance and with an approximately constant degree of superheat. However, performance degradation is important for significantly low charge levels (below 70% of the nominal charge), and the degree of superheat increases since, in this condition, the valve is fully open (Kim and Braun, 2012). Similar results were obtained by other authors (Farzad and O'Neal, 1994; Choi and Kim, 2004; Fernando et al., 2004) for systems equipped with an

* Corresponding author.
E-mail address: chiara.dignazi@polimi.it (C. D'Ignazi).

https://doi.org/10.1016/j.ijrefrig.2024.09.022
Received 22 May 2024; Received in revised form 19 September 2024; Accepted 23 September 2024
Available online 3 October 2024
0140-7007/

Nomenclature

c_P	Isobaric heating capacity [J kg^{-1} K^{-1}]
f	Frequency [Hz]
h	Enthalpy [J kg^{-1}]
$\dot{m}$	Mass flow rate [kg s^{-1}]
$\dot{Q}$	Heat flow rate [W]
T	Temperature [K]
$\dot{W}$	Power [W]

Greek symbols

ρ	Density [kg m^{-3}]

Subscripts

$COMP$	Compressor
$COND$	Condenser
G	Water-ethylene glycol mixture
IN	Inlet
OUT	Outlet
R	Refrigerant
SAT	Saturation
SH	Superheat [K]
$SUBC$	Subcooling [K]
W	Water

Acronyms

$BPHE$	Brazed plate heat exchangers
COP	Coefficient of performance
EXV	Electronic expansion valve
FXO	Fixed orifice expansion valve
GHG	Greenhouse gases
HX	Heat exchanger
TEV	Thermostatic expansion valve

electronic expansion valve. Sieres et al. (2020) showed how a deviation in refrigerant charge from the optimal level influences the subcooling and superheat, as well as the COP, the heating capacity and the power absorbed by the compressor in an R407C liquid-to-water heat pump equipped with a TEV. As the refrigerant charge decreases, the subcooling is drastically reduced, reaching zero for a certain minimum charge level, while the degree of superheat increases significantly. Corberán et al. (2008) evaluated the influence of the refrigerant charge of a reversible water-to-water propane heat pump with a TEV in terms of performance, showing that the COP has a maximum as the refrigerant charge varies, whether the machine is operated in cooling or heating mode.

All previously mentioned studies refer to heat pumps without liquid receivers. Nowadays, however, The mentioned studies focus on heat pumps without liquid receivers. Currently, most machines are reversible; therefore, they are equipped with a liquid receiver to accommodate to refrigerant charge variation in the heat exchangers when the operation is reversed. This component ensures refrigerant in the liquid state at its outlet, allowing the expansion valve to work properly. Very few studies have focused on the effects of refrigerant charge on heat pumps with liquid receivers. This may be due to the fact that, as reported by Corberán and Gonzalvez (1998), it is typically considered that the presence of this element at the inlet of the expansion valve brings the refrigerant at the condenser outlet in saturated conditions. This implies that, as stated by Corberán et al. (2008), the receiver is considered only partially full of liquid refrigerant. Therefore, a variation in charge only affects the level of the liquid phase inside the receiver, and the performance of the machine is less sensitive to charge variation. However, as shown by Corberán (2010) and Guzzardi et al. (2022), the liquid receiver can accumulate subcooled refrigerant, and, in this case, the saturation condition at the outlet of the condenser is no longer imposed and a charge variation will affect the performance of the system. Yamanaka et al. (1997) integrated the liquid receiver into the condenser of a vapor compression cycle used in car air conditioning systems, highlighting that optimal performance was achieved with subcooled refrigerant at the condenser outlet.

This paper wants to contribute to this discussion by analyzing the effects of a decreasing refrigerant charge on the performance of a R513A water-to-water heat pump equipped with a large liquid receiver. The refrigerant inside the machine is progressively extracted in a controlled way to simulate refrigerant leakages occurring during normal lifespan, being the influence of this phenomenon highlighted considering some operating parameters such as COP, heating capacity, subcooling, operating pressures and expansion valve opening. It is worth specifying that in this study, "large liquid receiver" means that the liquid receiver has an internal volume that can hold as much as 63.6% of the overall refrigerant charge in nominal conditions (see Section 3).

2. Experimental set-up and methodology

2.1. Experimental set-up

The experimental set-up is shown in Fig. 1. It is described in detail in Colombo et al. (2020) and in Molinaroli et al. (2022), but for the sake of completeness a brief description follows. The information is taken from the aforementionend papers to which the interested reader is addressed to for a more in-depth description of the test rig. The set-up comprises a water-to-water heat pump with R513A as refrigerant. It features two EXV valves installed in parallel for system operation; however, in this work, only the higher capacity valve is utilized. Additionally, the system includes a 2.8 dm^3 liquid receiver at the condenser outlet, a variable speed reciprocating compressor with a displacement of 13.15 m^3 h at 50 Hz, a 2.33 dm^3 vapor accumulator at the compressor inlet, and a hermetic oil separator. Stainless steel brazed plate heat exchangers are used for the condenser (40 plates) and evaporator (30 plates). A 25.4% volume basis ethylene glycol–water mixture is used as the secondary fluid in the evaporator, while water is used in the condenser. The hot circuit gives heat to the cold circuit through a heat exchanger ("recuperator" in Fig. 1) while the thermal power unbalance between the condenser and the evaporator is compensated by an auxiliary chiller ("Auxiliary HX"). Two 500 dm^3 tanks are installed to guarantee a nearly constant temperature of the water and water-ethylene glycol mixture at their outlet.[1]

Refrigerant and secondary fluids temperatures and pressures are measured by various sensors at different points of the experimental setup as shown in Fig. 1, while the refrigerant mass flow rate and density measurement are carried out by a Coriolis mass flow meter located at the condenser outlet. The power absorbed by the compressor is also measured through a programmable power meter. The recording of the experimental data, the opening of the secondary circuit valves, the setting of compressor and pumps speed are carried out through a LabVIEW interface. Further details on the components and instrumentation used can be found in Tables 1 and 2, respectively, which are consistent with the components and instrumentation utilized in previous studies (Colombo et al., 2020 and in Molinaroli et al., 2022) involving the same machine.

[1] It is worth specifying that the RTDs used to measure the temperature of the refrigerant are not immersed in the refrigerant but are placed inside capillary tubes which are brazed on the external surface of the refrigerant pipes. This assembly is then insulated so that the capillary tube achieves a temperature very similar to that of the refrigerant pipe which, in turn, is very close to that of the flowing refrigerant. A thermal analysis with a FEM software confirms that the three temperatures (refrigerant, refrigerant pipe and capillary tube) are within 0.03 K in steady state conditions.

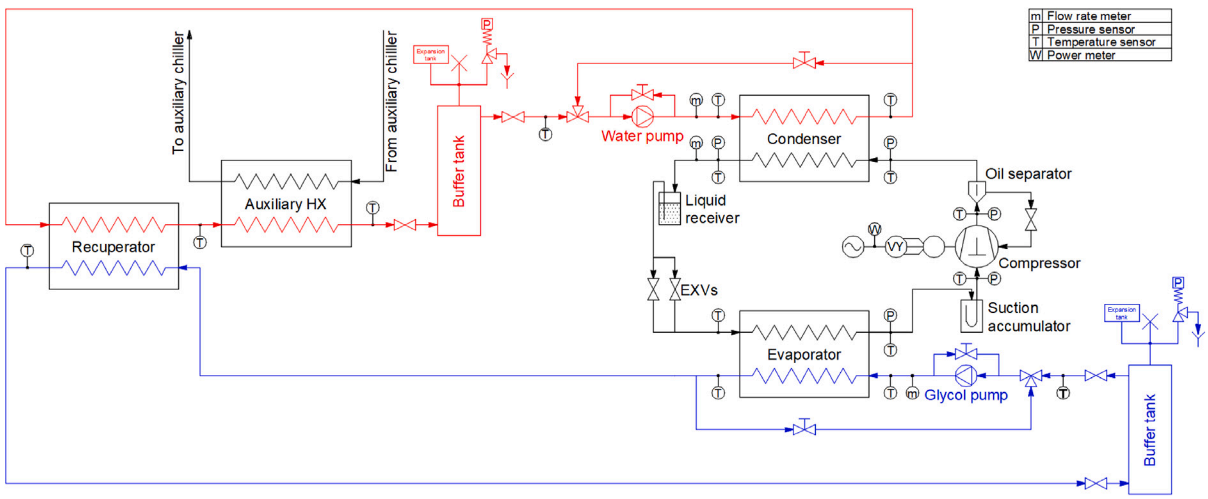

Fig. 1. Schematic of the experimental facility.

Table 1
Main characteristics of the components used in the experimental facility (Colombo et al., 2020; Molinaroli et al., 2022).

Component	Parameter	Range
Compressor	Swept volume @ 50 Hz	13.15 $m^3\ h^{-1}$
	Shaft rotational frequency	30 Hz–87 Hz
	Oil	POE ISO 32
	Oil charge	1.1 dm^3
Condenser	Height × Width × Depth	289 mm × 119 mm × 93.6 mm
	Number of plates	40
Evaporator	Height × Width × Depth	376 mm × 119 mm × 71.2 mm
	Number of plates	30
Expansion valve	Capacity range	1200 W–12 000 W
	Capacity range	1690 W–16 900 W
Liquid receiver	Volume	2.8 dm^3
Vapor accumulator at the compressor suction	Volume	2.33 dm^3
Oil separator	Type	Coalescence
	Volume	2.8 dm^3
Pumps (identical for both secondary fluid loops)	Nominal flow rate	28.7 $m^3\ h^{-1}$
	Nominal head	160 kPa
	Shaft rotational frequency	16 Hz–58 Hz
Recuperator	Height × Width × Depth	193 mm × 76 mm × 71.2 mm
	Number of plates	30

Table 2
Characteristics of the measuring instruments (Colombo et al., 2020 and Molinaroli et al., 2022).

Parameter	Instrument	Range	Accuracy
Refrigerant mass flow rate	Coriolis mass flow meter	0 kg h^{-1}–300 kg h^{-1}	±0.15 % r.v.
Refrigerant density	Coriolis mass flow meter	0 kg m^{-3}–2000 kg m^{-3}	±20 kg m^{-3}
Refrigerant pressure (low side)	Pressure transducer	0 kPa–700 kPa	±0.3 % f.s.
Refrigerant pressure (high side)	Pressure transducer	0 kPa–4000 kPa	±0.3 % f.s.
Refrigerant temperature	RTD Pt 100	243.15 K–373.15 K	±0.1 K
Compressor power	Power transducer	0 W–4000 W	±0.2 % f.s.
Water and water-ethylene glycol mass flow rate	Vortex flow meter	0.21 $m^3\ h^{-1}$–3 $m^3\ h^{-1}$	±2 % r.v.
Water and water-ethylene glycol temperature	RTD Pt 100	263.15 K–353.15 K	±0.1 K

2.2. Charging and discharging process

To identify the optimal refrigerant charge for the heat pump, the theoretical approach defined by Corberán et al. (2011) is used, according to which the maximum performance in terms of COP is obtained when the system works with a subcooling within 5–7 K. For this reason, the heat pump used for this experimental work is charged until reaching a subcooling of 6.86 K in nominal operating conditions (temperature of the water-ethylene glycol mixture at the evaporator inlet equal to 10 °C, temperature of the water at the condenser inlet and outlet equal to 40 °C and 45 °C respectively, target superheat equal to 5 K and compressor frequency equal to 50 Hz). As a result, the nominal refrigerant charge equals to 4680 g.

To simulate the refrigerant leakages, the following progressive discharging process is used:

1. Create vacuum inside a 128.55 cm^3 metal cylinder through a vacuum pump.
2. Weigh the cylinder on a precision scale to measure its tare.
3. Turn on the heat pump to allow the condensing and evaporating pressures to separate.

4. Use a flexible hose to connect the cylinder to the high-pressure or low-pressure side of the system to extract liquid or vapor phase refrigerant. The choice among liquid or vapor depends on how large the simulated leakage should be.
5. Weigh the metal cylinder and calculate the actual mass of refrigerant removed from the circuit.
6. Empty the metal cylinder and create a vacuum again.

This procedure is repeated until the desired refrigerant mass is removed from the heat pump. During the whole experimental campaign, the flexible hoses are kept connected to the refrigerant circuit. The hoses are equipped with two valves: one located between the system and the hose and the other at the end of the hose. The valve between the system and the hose is always kept closed, ensuring that there is no refrigerant flow between the system and the hose. The valve at the end of the hose is also kept closed when not in use. This configuration ensures that refrigerant remains trapped inside the hose between each charging cycle. The amount of refrigerant trapped in the hoses is estimated starting form their dimensions and the density of the refrigerant in vapor state or in liquid state, depending on the hose considered, in nominal operating conditions. It results in $0.21\,\mathrm{g}$ and $11.3\,\mathrm{g}$ respectively, i.e. around 0.23% of the nominal charge. As a result, with the first discharge a negligible reduction of the charge which is inside the heat pump has been created, being this reduction small enough not to significantly alter the performance of the heat pump. Additionally, it must be considered that during any discharging phase, this amount of refrigerant flows out of the hose to fill the metal cylinder and is replaced by fresh one which is still there during the next heat pump operation.

The main characteristics of the instruments used in the procedure described above are as follows:

- Copper cylinder, with an internal volume equal to 128.55 cm^3.
- Dual-stage vacuum pump, with a maximum flow rate of 42 $\mathrm{dm}^3\ \mathrm{h}^{-1}$ and maximum vacuum level of 2 Pa.
- Precision scale, with maximum capacity of 3200 g and 0.01 g resolution.

2.3. Test procedure and data reduction

The heat pump is tested in steady-state condition for different refrigerant charges. The steady-state condition is guaranteed if the maximum mean deviation of each temperature and pressure measurement is lower than 0.2 K and 2.5 kPa respectively for a time span of 900 s. Once the stability is reached, measurements are taken for additional 900 s with a sampling rate of 1 Hz. During this second time interval the stability of each measurement is checked and, in order for the test to be valid, has to be maintained. During the tests, the secondary fluids flow rates and temperatures are controlled acting on the two and three-way valves (see Fig. 1 for their position) and on the rotational speed of the pumps.

Regarding the data reduction, differently from our previous studies (Colombo et al., 2020; Molinaroli et al., 2022), the heat pump heating capacity $\dot{Q}_{COND}$ is determined on the water side only to improve the measurement accuracy. Indeed, as shown in the next section, at low charge operating conditions a two-phase flow of refrigerant at condenser outlet may occur, resulting in a difficult estimate of the enthalpy from pressure and temperature measurements. The equation for the capacity calculation is the following:

$$\dot{Q}_{COND} = \dot{m}_W \left[c_{P,W} \left(T_{W,OUT,COND} - T_{W,IN,COND}\right)\right] \tag{1}$$

The Coefficient Of Performance (COP) is calculated as follows, and the power of the compressor is measured before the inverter.

$$COP = \frac{\dot{Q}_{COND}}{\dot{W}_{COMP}} \tag{2}$$

The subcooling is calculated according to Eq. (3). Notably, the temperature at the condenser outlet is directly measured via a sensor, while the saturation temperature is calculated from the saturation tables of the refrigerant R513A available through Refprop 10 (Lemmon et al., 2018).

$$\Delta T_{SUBC} = T_{SAT}(p_{OUT,COND}) - T_{OUT,COND} \tag{3}$$

Finally, as indicated by ISO/IEC GUIDE 98-3:2008 (JCGM, 2008), the uncertainty of each directly measured parameter is evaluated considering both the accuracy of the sensor used to measure it and the standard deviation of the mean value. For the calculated parameters, the error propagation equation is used to estimate the uncertainty. The level of confidence for both kind of parameters is 95%. The uncertainty of the heating capacity ranges from 1.45% to 2.51%while that of the COP varies from 1.49% to 2.55%.

3. Results and discussion

3.1. Description of laboratory tests

An analysis of how the refrigerant charge impacts the heat pump's performance is conducted, taking into account three different test types outlined in Table 3 at different charge levels.

The analysis of the influence of the refrigerant charge on the performance of the heat pump is carried out considering three different groups of tests as shown in Table 3. First, a reference condition is chosen to identify the charge of the refrigerant and the flow rates of the two secondary fluids that flow through the evaporator and the condenser. From these fluids perspective, this test is carried out setting the water temperature at the condenser outlet to 45 °C, the water-ethylene glycol mixture temperature at the evaporator inlet to 10 °C, and changing the flow rates so that temperature variations equal to 5 K across the two heat exchangers are found. From the refrigerant point of view, this test is run setting the rotational frequency of the compressor shaft to 50 Hz, the superheating at the evaporator outlet to 5 K and looking for a charge that leads to a subcooling at condenser outlet in the range between 5 K and 7 K, as explained in Section 2.2. The final charge results in 4680 g and the corresponding subcooling is 6.86 K. Then, three different kinds of tests are carried out:

1. T1 tests: in these tests the flow rate of the secondary fluids in the evaporator and condenser is fixed, the water temperature at the condenser outlet is set to 45 °C and the water-ethylene glycol mixture temperature at the evaporator inlet is set to 0 °C, 5 °C, 10 °C, 15 °C, 20 °C. The water temperature at the condenser inlet and the water-ethylene glycol temperature at evaporator outlet change according to the different operating condition of the heat pump. In each test, the rotational frequency of the compressor shaft is fixed to 50 Hz.
2. T2 tests: in these tests, the temperatures of the secondary fluids entering and exiting from both the evaporator and condenser are set, specifically at 10 °C and 5 °C in the evaporator, and at 40 °C and 45 °C in the condenser. As a result, according to the different operating condition of the heat pump, their flow rate is varied accordingly. In each test, the rotational frequency of the compressor shaft is fixed to 50 Hz.
3. T3 tests: in these tests the flow rates of the secondary fluids are fixed at the values corresponding to the reference conditions. The water temperatures at the condenser inlet and outlet are set to 40 °C and 45 °C, respectively. The water-ethylene glycol mixture temperature at the evaporator inlet is set to 0 °C, 5 °C, 10 °C, 15 °C, 20 °C, while the temperature at the evaporator outlet changes according to the different operating condition of the heat pump. The rotational frequency of the compressor shaft is varied to accommodate to the different refrigerant charges.

Table 3
Experimental conditions.

Test	Charge	f_{COMP}	Evaporator			Condenser		
			$\dot{m}_G$	$T_{G,IN}$	$T_{G,OUT}$	$\dot{m}_W$	$T_{W,IN}$	$T_{W,OUT}$
		[Hz]	[kg/h]	[°C]	[°C]	[kg/h]	[°C]	[°C]
Reference	4680	50	Identified	10	5	Identified	40	45
T1	35%–100%	50	As reference	0-5-10-15-20	–	As reference	–	45
T2	35%–100%	50	Identified	10	5	Identified	40	45
T3	35%–100%	Identified	As reference	0-5-10-15-20	–	As reference	40	45

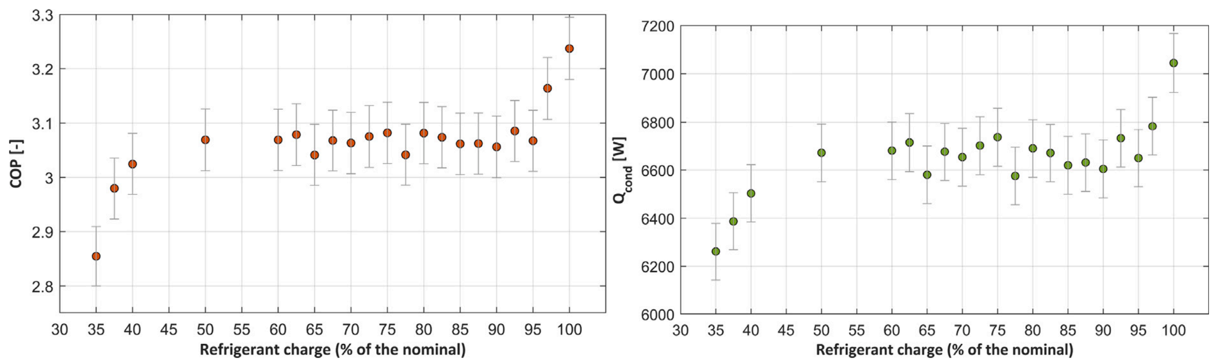

Fig. 2. COP (left) and heating capacity (right) as a function of the refrigerant charge for T1 tests with $T_{G,IN,EVAP}$ = 10 °C, $\dot{m}_{G,EVAP}$ = 1100 kg/h and $\dot{m}_{W,COND}$ = 1200 kg/h.

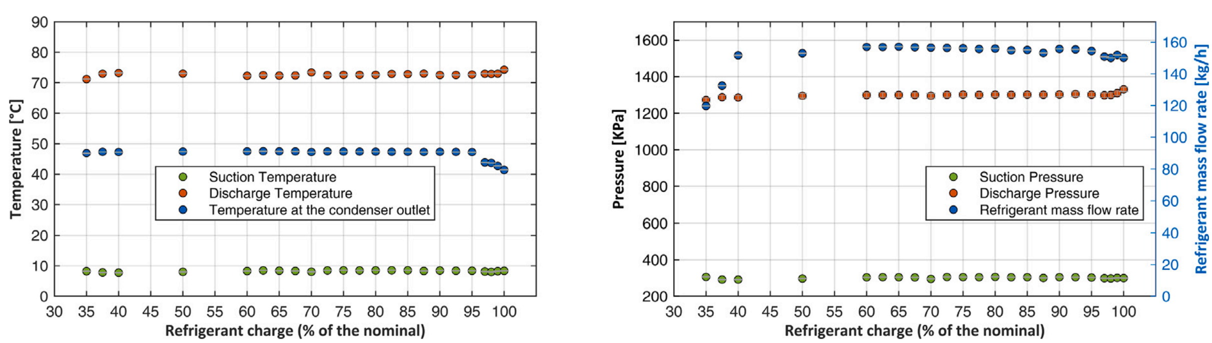

Fig. 3. Refrigerant temperatures at compressor suction, compressor discharge and condenser outlet (left) and pressures at the compressor suction and discharge as well as refrigerant mass flow rate (right) as a function of the refrigerant charge for T2 and with $\dot{m}_{G,EVAP}$ between 900 kg/h and 1100 kg/h and $\dot{m}_{W,COND}$ in the range 1050 kg/h to 1200 kg/h.

3.2. Results

Starting from the heat pump "macroscopic" performance, Fig. 2 shows the *COP* and the heating capacity as a function of the R513A charge for the T1 tests. Both the *COP* and the heating capacity reach a maximum at the nominal charge (100%) as the heat pump was charged with an amount of refrigerant to maximize performance, as explained in Section 2.2. Then, as the charge decreases, first a steep reduction of these parameters is observed in the range of charge 95%–100%, then a plateau in the range of charge 40%–95% is found and, finally, a sharp drop is measured when the charge is below 40% of the nominal one.

A similar trend is reported for the thermodynamic parameters, i.e. refrigerant pressures at compressor suction and discharge, refrigerant temperatures at compressor suction, compressor discharge and condenser outlet and refrigerant mass flow rate, as shown in Fig. 3. Indeed, in the range of charge 40%–95% these parameters are almost constant while, outside this range, they change as the refrigerant charge decreases, with a very high slope for extremely low charges (35%–40%).

An insight on the variation of the subcooling at the condenser outlet with the refrigerant charge for T2 tests is shown in Fig. 4. As long as positive, the subcooling is one of the most affected quantities by a refrigerant charge variation since it sharply reduces from the nominal value to 0 K as the charge is extracted from the heat pump. For charge level below 95% of the nominal charge (i.e. below 4454 g in the system used in the present study), the subcooling becomes equal to 0 K in the full range of refrigerant charge analyzed. This means that there exists a threshold value of the charge below which the refrigerant at the outlet of the condenser is no longer subcooled, being also possible that the condensation is not completely attained.

A direct proof of this consideration is found in Fig. 5 in which the density of the refrigerant at the outlet of the condenser that is measured by the Coriolis mass flow meter is reported as a function of the refrigerant charge. From the analysis of this figure it is possible to highlight that, when there is not any subcooling, the refrigerant density at the outlet condenser may be lower than the saturated liquid density at condensing pressure, i.e. the refrigerant is in a two-phase state and the full condensation is not attained.[2] On the other hand, when there is subcooling, the density of the refrigerant is greater than the density of the saturated liquid at the condensing pressure since the temperature of the refrigerant is lower than the temperature of the saturated liquid

[2] Authors are aware that the measurement of the mass flow rate and density by Coriolis flow meter may be inaccurate. However, in this study the information is used to qualitatively check that the refrigerant at the outlet of the condenser is in a two-phase state because the use of pressure and temperature does not provide any useful information about it.

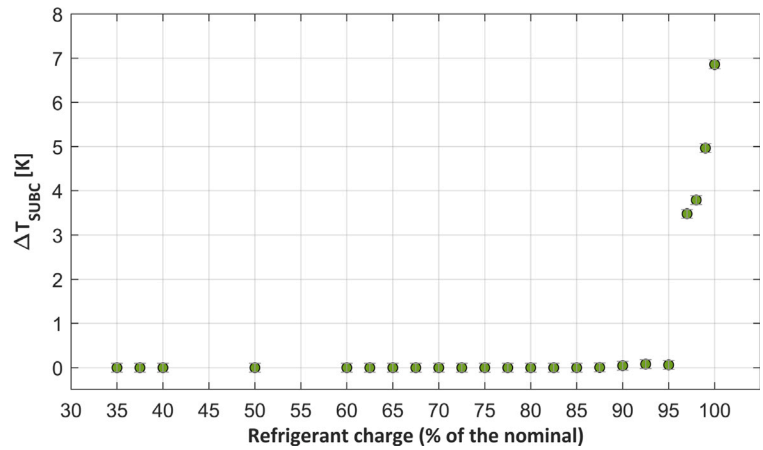

Fig. 4. Subcooling as a function of the charge, $T_{G,IN,EVAP}$ = 10 °C (T2 tests).

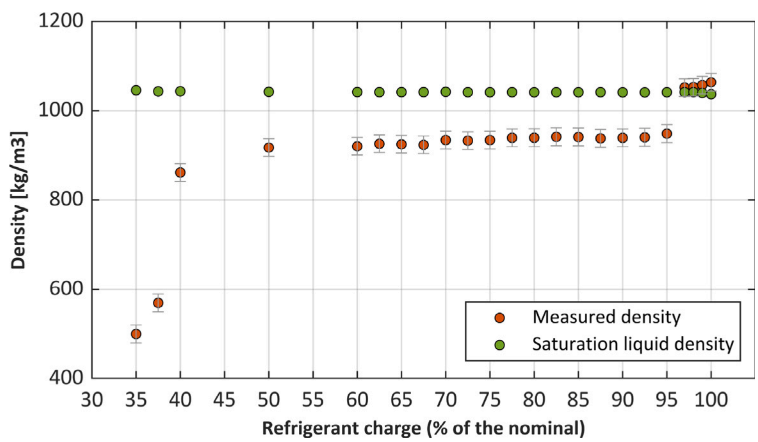

Fig. 5. Density of the refrigerant at the condenser outlet as a function of the charge, $T_{G,IN,EVAP}$ = 10 °C (T2 tests).

at the same pressure and the thermal expansion coefficient of R513A, as computed with Refprop 10.0 (Lemmon et al., 2018), is positive.

Overall for most of the operating parameters of the heat pump it is possible to identify three different zones as the charge decreases: "positive subcooling" zone (first zone, range of charge: 95%–100%), "plateau" zone (second zone, range of charge: 40%–95%), and "compressor failure risk" zone (third zone, range of charge range: below 40%). In the first zone, the reduction of the refrigerant charge directly affects the heat pump operation leading to a degradation of its performance. In this zone, as the charge reduces, the subcooling reduces but subcooled refrigerant is still found at condenser outlet. This means that the liquid receiver is completely filled by subcooled refrigerant. In the intermediate zone, also referred to as the "plateau", the operation of the heat pump is not affected by the reduction of the refrigerant charge. This is the range of refrigerant charge in which the presence of the liquid receiver is fundamental for the correct operation of the heat pump. Indeed, in this range of charge, there is not any subcooling, and a two-phase flow is likely to be found at the condenser outlet, but the liquid receiver ensures that the refrigerant remains in the saturated liquid state at its outlet, allowing for the correct feeding and operation of the expansion valve. In this range of charge, the only parameters that varies is the amount of saturated vapor inside the liquid receiver: the lower is the charge, the higher is the volume filled by the vapor inside the liquid receiver. Below 40% of the nominal charge, the liquid receiver does not hold any liquid refrigerant and it cannot work as a liquid refrigerant buffer anymore. As a result, a two-phase flow feeds the EXV which, due to the presence of bubbles at its inlet (Fig. 7), does not operate appropriately. Indeed, the opening of the EXV (Fig. 6) increases until its maximum value and the superheating at evaporator outlet increases too, up to 13.1 K.

A similar behavior at low charges was found by Kim and Braun (2012). This operating zone is particularly dangerous for the compressor since it operates with low suction pressure, high pressure ratio and very high temperature of the refrigerant at its discharge, resulting in a possible failure related to lubricant thermal decomposition. It is worth noting that, in authors' thought, this behavior is general and valid for any heat pump equipped with a liquid receiver, but the charge thresholds that separate the three above mentioned zones are specific for each system since they depend on the features of the components, especially on the liquid receiver volume. However, the refrigerant charge at which the transition from the second zone ("plateau") to the third zone ("compressor failure risk") can be roughly estimated considering the reference testing condition (see 3). Under nominal charging conditions (100%, 4680 g), a density of the refrigerant at the condenser outlet equal to 1063.79 $\mathrm{kg\,m^{-3}}$ is measured; considering that the liquid receiver volume is 2.8 $\mathrm{dm^3}$, the mass of refrigerant stored in

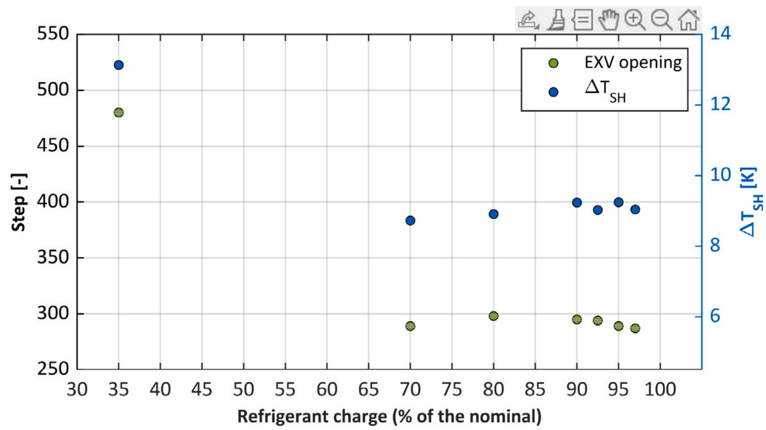

Fig. 6. EXV opening and superheating at the outlet of the evaporator as function of the charge for T1 tests with $T_{G,IN,EVAP}$ = 20 °C, $\dot{m}_{G,EVAP}$ ≈ 1100 kg/h and $\dot{m}_{W,COND}$ ≈ 1200 kg/h.

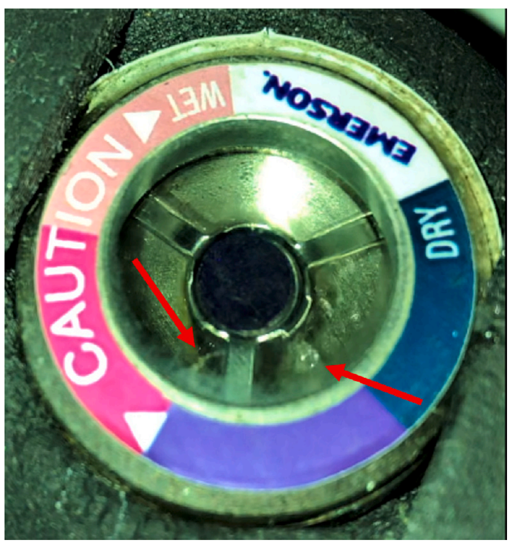

Fig. 7. Bubbles at EXV inlet.

it is equal to 2978 g, i.e. around 64% of the overall refrigerant charge, which is the reason why the liquid receiver is considered "large" . As a result, if the heat pump contains less than 1702 g of refrigerant, liquid is not present in the liquid receiver anymore and, therefore, it is not possible to correctly feed the expansion valve. An amount of 1702 g of refrigerant corresponds to 36.32% of the nominal charge, which is very close to the experimentally found threshold that separates the second zone from the third zone.

Finally, the influence of the refrigerant charge on the rotational frequency of the compressor shaft is assessed with the aim of achieving a constant heating capacity. The results are shown in Fig. 8 and demonstrate that, to keep the heating capacity constant, the required rotational frequency has to increase as the refrigerant charge decreases. In the range between 92.5% and 70% of the nominal charge the frequency is nearly constant due to the liquid receiver influence whereas it has to increase up to the value of 60 Hz at 35% of charge.

4. Conclusions

In this paper, the results of an experimental analysis of the effects of a decreasing refrigerant charge on the performance and operating conditions of an R513A water-to-water heat pump equipped with a large liquid receiver, an electronic valve, and a variable speed compressor are discussed.

The heat pump is tested in steady-state conditions with three different testing procedures to highlight how the "macroscopic" parameters (COP and heating capacity), on the "thermodynamic parameters" (pressures and temperatures) and on the "components parameters" (opening of the EXV, rotational frequency of the compressor shaft) change as a function of the refrigerant charge.

The results show a peculiar trend for almost all parameters as the charge level decreases since it is possible to identify three different ranges of charge in which their trends change. In the first zone ("positive subcooling" zone, range of charge 95%–100% for the heat pump considered in this study) all the parameters change since the heat pump operates with a subcooling that is approaching 0 K as the refrigerant charge reduces. In the second zone ("plateau" range of charge 40%–95% for the heat pump considered in this study) all the parameters are nearly constant since the liquid receiver allows to feed the EXV with saturated liquid. In the third zone ("compressor failure risk", range of charge below 40% for the heat pump considered in this study) all the parameters exhibit a sudden change since the EXV operates with two-phase flow at its inlet and it is not able to keep the superheating at the target value anymore. It is the authors' thought that this behavior is generally valid for any heat pump equipped with a liquid receiver, being the threshold values of the refrigerant charge that separate each zone different form system to system and largely related to the size of the liquid receiver.

Overall, the following conclusions can be drawn from this study:

- The presence of subcooled refrigerant at the condenser outlet indicates normal operation of the heat pump, whereas saturated liquid condition may be acceptable if it is intentional and there is not any refrigerant leak. However, if it is due to a leak, it will eventually lead to the heat pump operating in third zone.
- The refrigerant subcooling at the condenser outlet is a good predictor of the charge level as long as it is greater than 0 K. Since this parameter can be easily measured using conventional pressure and temperature instrumentation, it should be among those monitored by Fault Detection and Diagnosis algorithms. However, when the subcooling is zero, it becomes impossible to draw information from pressure and temperature measurements as these parameters remain constant whatever is the amount of refrigerant in liquid state inside the receiver. In this situation, it is advisable to use a liquid-level sensor to monitor the refrigerant level and understand if the heat pump operation safely and firmly in the second zone or if it is approaching the third zone.
- The operation in third zone is problematic as it can cause damage to the compressor. This condition can be detected by measuring superheating through pressure and temperature measurements or by evaluating the refrigerant vapor quality at the expansion valve inlet.

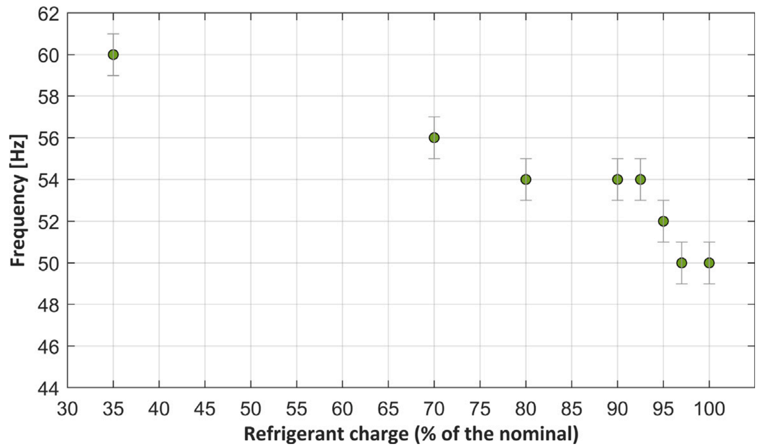

Fig. 8. Compressor frequency over refrigerant charge, $T_{G,IN,EVAP}$ = 10 °C, $\dot{m}_{G,EVAP}$ = 1100 kg/h and $\dot{m}_{W,COND}$ = 1200 kg/h (T3 tests).

CRediT authorship contribution statement

Chiara D'Ignazi: Writing – original draft, Methodology, Investigation, Formal analysis, Data curation, Conceptualization. **Luca Molinaroli:** Writing – review & editing, Supervision, Methodology. **Carla Bongiorno:** Methodology, Investigation, Formal analysis, Data curation, Conceptualization.

Declaration of competing interest

The authors declare that they have no known competing financial interests or personal relationships that could have appeared to influence the work reported in this paper.

References

Choi, J., Kim, Y., 2004. Influence of the expansion device on the performance of a heat pump using R407c under a range of charging conditions. Int. J. Refrig. 27, 378–384.

United Nations Framework Convention on Climate Change, 2015. Paris agreement. In: Report of the Conference of the Parties To the United Nations Framework Convention on Climate Change. p. 2017, (21st Session, 2015: Paris). Retrived December, HeinOnline..

Colombo, L.P.M., Lucchini, A., Molinaroli, L., 2020. Experimental analysis of the use of R1234yf and R1234ze(E) as drop-in alternatives of R134a in a water-to-water heat pump. Int. J. Refrig. 115, 18–27.

Corberán, J.M., 2010. Role, sizing and influence of the liquid receiver. In: IIR 2nd Workshop on Refrigerant Charge Reduction.

Corberán, J., Gonzalvez, J., 1998. The matching problem on the modeling of vapor compression systems. In: Proceedings of the International Refrigeration and Air Conditioning Conference. p. 416.

Corberán, J.M., Martínez, I.O., Gonzálvez, J., 2008. Charge optimisation study of a reversible water-to-water propane heat pump. Int. J. Refrig. 31, 716–726.

Corberán, J.M., Martínez-Galván, I., Martínez-Ballester, S., Gonzálvez-Maciá, J., Royo-Pastor, R., 2011. Influence of the source and sink temperatures on the optimal refrigerant charge of a water-to-water heat pump. Int. J. Refrig. 34, 881–892.

Du, Z., Domanski, P.A., Payne, W.V., 2016. Effect of common faults on the performance of different types of vapor compression systems. Appl. Therm. Eng. 98, 61–72.

European Commission, In focus: Energy efficiency in buildings URL: https://ec.europa.eu/info/news/focus-energy-efficiency-buildings-2020-lut-17_en.

Farzad, M., O'Neal, D., 1994. The effect of improper refrigerant charging on the performance of a residential heat pump with fixed expansion devices (capillary tube and short tube orifice). In: Proceedings of Intersociety Energy Conversion Engineering Conference. p. 3836.

Fernando, P., Palm, B., Lundqvist, P., Granryd, E., 2004. Propane heat pump with low refrigerant charge: design and laboratory tests. Int. J. Refrig. 27, 761–773.

Grace, I., Datta, D., Tassou, S., 2005. Sensitivity of refrigeration system performance to charge levels and parameters for on-line leak detection. Appl. Therm. Eng. 25, 557–566.

Guzzardi, C., Azzolin, M., Lazzarato, S., Del Col, D., 2022. Refrigerant mass distribution in an invertible air-to-water heat pump: effect of the airflow velocity. Int. J. Refrig. 138, 180–196.

Houcek, J., Thedford, M., 1984. A research into a new method of refrigeration charging and the effects of improper charging. In: Proceedings of the First Symposium on Improving Building Systems in Hot and Humid Climates. Energy Systems Laboratory, http://esl.tamu.edu.

JCGM, 2008. Evaluation of Measurement Data—Guide to the Expression of Uncertainty in Measurement. 50, Int. Organ. Stand., Geneva ISBN, 134.

Kim, W., Braun, J.E., 2012. Evaluation of the impacts of refrigerant charge on air conditioner and heat pump performance. Int. J. Refrig. 35, 1805–1814.

Lemmon, E., Bell, I., Huber, M., McLinden, M., 2018. NIST Reference Fluid Thermodynamic and Transport Properties Database (REFPROP), Version 10.0; StAndaRd Reference Data. National institute of standards and technology, Gaithersburg, md, pp. 288–290, NIST Stand. Ref. Databasev23.

Molinaroli, L., Lucchini, A., Colombo, L.P.M., 2022. Drop-in analysis of R450A and R513A as low-gwp alternatives to R134a in a water-to-water heat pump. Int. J. Refrig. 135, 139–147.

Sieres, J., Ortega, I., Cerdeira, F., Álvarez, E., 2020. Influence of the refrigerant charge in an R407C liquid-to-water heat pump for space heating and domestic hot water production. Int. J. Refrig. 110, 28–37.

Yamanaka, Y., Matsuo, H., Tuzuki, K., Tsuboko, T., Nishimura, Y., 1997. Development of sub-cool system. SAE Trans. 106, 129–134, URL: http://www.jstor.org/stable/44731167.